Addition of Small Molecules to $(\eta\text{-}C_5H_5)_2Rh_2(\mu\text{-}CO)(\mu\text{-}CF_3C_2CF_3)$. 7.[1] Formation and Properties of Several Isocyanide Complexes $(\eta\text{-}C_5H_5)_2Rh_2(CO)(CNR)(\mu\text{-}CF_3C_2CF_3)$, Crystal and Molecular Structure of the Complex with R = 2,6-$Me_2C_6H_3$, and Structure and Substituent Influences on the Electrochemistry of $(\eta\text{-}C_5H_5)_2Rh_2(CO)L(\mu\text{-}CF_3C_2CF_3)$ (L = CO, PPh_3, or CN-*t*-Bu)

John W. Bixler,[2,3] Alan M. Bond,*[2] Ron S. Dickson,*[4] Gary D. Fallon,[4] Rhonda J. Nesbit,[4] and Helen Pateras[4]

Division of Chemical and Physical Sciences, Deakin University, Waurn Ponds, Victoria 3217, Australia, and Department of Chemistry, Monash University, Clayton, Victoria 3168, Australia

Received March 25, 1987

The isocyanides CNR (R = Et, *i*-Pr, Cy, 2,6-$Me_2C_6H_3$) add coordinatively to $(\eta\text{-}C_5H_5)_2Rh_2(\mu\text{-}CO)(\mu\text{-}CF_3C_2CF_3)$ to give $(\eta\text{-}C_5H_5)_2Rh_2(CO)(CNR)(\mu\text{-}CF_3C_2CF_3)$. Spectroscopic results indicate that the CO and CNR ligands are both terminal. The complexes with R = Et, *i*-Pr, and Cy rearrange to isomeric species when left in solution, but those with R = 2,6-$Me_2C_6H_3$ and *t*-Bu are stable to this rearrangement. The structure of the complex with R = 2,6-$Me_2C_6H_3$ has been determined by X-ray crystallography. Crystal data: $C_{24}H_{19}F_6NORh_2$, M_r 657.9, orthorhombic, *Pbca*, a = 17.950 (8) Å, b = 17.161 (8) Å, c = 15.273 (7) Å, Z = 8, final R = 0.061 for 2306 "observed" reflections. The molecular structure reveals a trans arrangement of the CO and CNR ligands and an orientation of the alkyne parallel to the Rh–Rh bond. The electrochemical behavior of several complexes $(\eta\text{-}C_5H_5)_2Rh_2(CO)L(\mu\text{-}CF_3C_2CF_3)$ (L = CO, CN-*t*-Bu, PPh_3) has been determined and contrasted with that already reported for $(\eta\text{-}C_5H_5)_2Rh_2(\mu\text{-}CO)(\mu\text{-}CF_3C_2CF_3)$. Reduction and oxidation of $(\eta\text{-}C_5H_5)_2Rh_2(CO)_2(\mu\text{-}CF_3C_2CF_3)$ are both more difficult to achieve than with $(\eta\text{-}C_5H_5)_2Rh_2(\mu\text{-}CO)(\mu\text{-}CF_3C_2CF_3)$, and most of the redox intermediates formed are unstable. With $(\eta\text{-}C_5H_5)_2Rh_2(CO)_2(\mu\text{-}CF_3C_2CF_3)$, the reduction and oxidation pathways are critically dependent on the orientation of the carbonyl groups. Oxidation of $(\eta\text{-}C_5H_5)_2Rh_2(CO)L(\mu\text{-}CF_3C_2CF_3)$ (L = CN-*t*-Bu, PPh_3) leads to numerous pathways for rearrangement after electron transfer and to the formation of electrode- and solvent-dependent redox behavior. Chemical oxidation of the complexes $(\eta\text{-}C_5H_5)_2Rh_2(CO)(CNR)(\mu\text{-}CF_3C_2CF_3)$ with Me_3NO gives the bridging acrylamide complexes $(\eta\text{-}C_5H_5)_2Rh_2\{\mu\text{-}\eta^3\text{-}N(R)C(O)C(CF_3)C(CF_3)\}$. The same complexes are obtained upon treatment of $(\eta\text{-}C_5H_5)_2Rh_2(CO)_2(\mu\text{-}CF_3C_2CF_3)$ with the isocyanates RNCO (R = Me, *t*-Bu, *p*-MeC_6H_4).

Introduction

In previous papers, we described the formation of the isocyanide complex $(\eta\text{-}C_5H_5)_2Rh_2(CO)(CN\text{-}t\text{-}Bu)(\mu\text{-}CF_3C_2CF_3)$[5] and its oxidation with trimethylamine *N*-oxide to the bridging acrylamide complex $(\eta\text{-}C_5H_5)_2Rh_2\{\mu\text{-}\eta^3\text{-}N(t\text{-}Bu)C(O)C(CF_3)C(CF_3)\}$.[6] We also reported that the complexes $(\eta\text{-}C_5H_5)_2Rh_2(CO)(CNR)(\mu\text{-}CF_3C_2CF_3)$ and $(\eta\text{-}C_5H_5)_2Rh_2\{\mu\text{-}\eta^3\text{-}N(R)C(O)C(CF_3)C(CF_3)\}$ were both formed when $(\eta\text{-}C_5H_5)_2Rh_2(\mu\text{-}CO)(\mu\text{-}CF_3C_2CF_3)$ was treated with carbodiimides, RNCNR (R = *i*-Pr, Cy).[6] In isolating the isocyanide complexes, we recognized that some of them transformed in solution to a new species that seemed to be an isomer of the initial complex. In the following paper,[7] we describe our detailed investigation of these isomeric products. This paper is concerned with the formation and structural characterization of the complexes $(\eta\text{-}C_5H_5)_2Rh_2(CO)(CNR)(\mu\text{-}CF_3C_2CF_3)$ and with a comparison of the electrochemical properties of several complexes $(\eta\text{-}C_5H_5)_2Rh_2(CO)L(\mu\text{-}CF_3C_2CF_3)$ (L = CO, CN-*t*-Bu, PPh_3).

Experimental Section

General Procedures. All preparations were performed under an atmosphere of purified nitrogen by using Schlenk-type apparatus[8] or Pyrex Carius tubes. Preparative-scale thin-layer chromatography was carried out on 20 by 20 cm plates with a 1:1 silica gel G–HF_{254} mixture as adsorbent. All separations were achieved on deactivated plates, obtained by drying at room temperature only. Microanalyses were performed by the Australian Microanalytical Service, Melbourne, Australia. Melting points are uncorrected.

Instrumentation. Infrared absorption spectra were recorded on Jasco IRA 1 and A 100 spectrometers using KBr pellets or matched 0.1-mm sodium chloride solution cells. A V.G. Micromass 70/70-F spectrometer was used to record the mass spectra; the spectrometer was operated at 70 eV and 200 °C inlet temperature. NMR spectra were measured on a Brüker WH-90 or AM-300 spectrometer. The ^1H NMR spectra were measured at 90 or 300 MHz, ^{19}F at 84.7 or 282.4 MHz, and ^{13}C at 75.5 MHz; deuteriated solvents ($CDCl_3$, acetone-d_6) were used as internal locks. Chemical shifts are in parts per million from internal Me_4Si for ^1H and ^{13}C and from CCl_3F for ^{19}F; in all cases, a positive chemical shift denotes a resonance downfield from the reference. In ^{13}C spectra, $Cr(acac)_3$ was added to reduce T_1 relaxation times for carbonyl-containing compounds.

Electrochemistry. Working electrodes included a 4.5-mm diameter stationary platinum disk, a Beckman variable-speed rotated platinum disk, a Metrohm micrometer-style hanging mercury drop electrode, and a dropping mercury electrode mounted onto a Princeton Applied Research Corp. (PARC) 174/70 drop timer. The auxiliary electrode was a platinum wire. The

(1) Part 6: Dickson, R. S.; Fallon, G. D.; Jenkins, S. M.; Nesbit, R. J. *Organometallics* **1987**, *6*, 1240.
(2) Deakin University.
(3) On leave from State University College at Brockport, Brockport, NY 14420.
(4) Monash University.
(5) Dickson, R. S.; Oppenheim, A. P.; Pain, G. N. *J. Organomet. Chem.* **1982**, *224*, 377.
(6) Dickson, R. S.; Nesbit, R. N.; Pateras, H.; Baimbridge, W. *Organometallics* **1985**, *4*, 2128.
(7) Dickson, R. S.; Fallon, G. D.; Nesbit, R. J.; Pateras, H. *Organometallics*, following paper in this issue.
(8) Shriver, D. F.; Drezdzon, M. A. *The Manipulation of Air-Sensitive Compounds*, 2nd ed.; Wiley-Interscience: New York, 1986.

0276-7333/87/2306-2508$01.50/0

reference electrode was either Ag/AgCl (acetone, saturated with dry LiCl) or Ag/$AgNO_3$ (0.01 M) in acetonitrile containing 0.1 M Et_4NClO_4. Voltammetric and polarographic data were obtained by using a PARC 174A polarographic analyzer equipped with a Houston 2000 recorder or a Bioanalytical Systems BAS-100 electrochemical analyzer. Controlled potential electrolyses were carried out at a massive platinum gauze working electrode, using a PARC 173/179 potentiostat/digital coulometer.

Solvents, Ligands, and Reagents. Acetone was analytical grade reagent; pentane, hexane, and dichloromethane were purified by standard procedures.[9] "X4" refers to petroleum fraction of boiling point range 30–60 °C. All solvents were stored in the dark over activated 4A molecular sieves. The following isocyanide and isocyanate ligands were obtained commercially and were used without purification: *t*-BuNC, CyNC, *i*-PrNC, MeNCO (Strem), *p*-MeC_6H_4NCO (EGA). Trimethylamine *N*-oxide (EGA) was dehydrated by sublimation at 120 °C under vacuum. Literature procedures were used to prepare the following compounds: $(\eta\text{-}C_5H_5)_2Rh_2(CO)_2(\mu\text{-}CF_3C_2CF_3)$,[10] $(\eta\text{-}C_5H_5)_2Rh_2(\mu\text{-}CO)(\mu\text{-}CF_3C_2CF_3)$,[5] $(\eta\text{-}C_5H_5)_2Rh_2(CO)(CN\text{-}t\text{-}Bu)(\mu\text{-}CF_3C_2CF_3)$,[5] $(\eta\text{-}C_5H_5)_2Rh_2(CO)(PPh_3)(\mu\text{-}CF_3C_2CF_3)$,[5] EtNC,[11] and 2,6-$Me_2C_6H_3NC$.[12]

Reaction of $(\eta\text{-}C_5H_5)_2Rh_2(\mu\text{-}CO)(\mu\text{-}CF_3C_2CF_3)$ (1) with RNC. EtNC. A slight excess of ethyl isocyanide (0.010 g) was added to a solution of **1** (0.091 g, mole ratio = 1:1) in dichloromethane (10 mL) at 20 °C. There was an immediate color change from green to orange. Removal of solvent and excess ligand under vacuum and TLC of the orange residue with 1:1 X4/CH_2Cl_2 as eluent separated a major orange product from a minor orange-red compound. It was difficult to obtain pure samples of the major product in this manner because it converted continuously in solution to the minor product. This problem was overcome by pouring a fresh reaction solution into pentane. This gave orange crystals of $(\eta\text{-}C_5H_5)_2Rh_2(CO)(CNEt)(\mu\text{-}CF_3C_2CF_3)$ (0.095 g, 95%), mp 99 °C. Anal. Calcd for $C_{18}H_{15}F_6NORh_2$: C, 37.2; H, 2.6; F, 19.6. Found: C, 37.2; H, 2.6; F, 20.1. Spectroscopic data: IR (CH_2Cl_2) ν(CN) at 2170 vs, ν(CO) at 1990 vs, ν(C=C) at 1630 m cm^{-1}; ^1H NMR ($CDCl_3$) δ 5.39 (s, 10 H, 2 × C_5H_5), 3.66 (q, 2 H, J = 7 Hz, CH_2), 1.35 (t, 3 H, J = 7 Hz, CH_3); ^{19}F NMR ($CDCl_3$) δ −54.9 (s); MS, m/z (relative intensity) 581 $[M]^+$ (1), 553 $[M - CO]^+$ (13), 534 $[M - CO - F]^+$ (2), 526 $[M - CNEt]^+$ (3), 233 $[C_{10}H_{10}Rh]^+$ (100).

***i*-PrNC.** In similar manner, **1** (0.090 g) and isopropyl isocyanide gave orange crystals of $(\eta\text{-}C_5H_5)_2Rh_2(CO)(CN\text{-}i\text{-}Pr)(\mu\text{-}CF_3C_2CF_3)$ (0.097 g, 95%), mp 82 °C. Anal. Calcd for $C_{19}H_{17}F_6NORh_2$: C, 38.3; H, 2.9; F, 19.2. Found: C, 38.3; H, 3.0; F, 18.8. Spectroscopic data: IR (CH_2Cl_2) ν(CN) at 2155 vs, ν(CO) at 1990 vs, ν(C=C) at 1640 m cm^{-1}; IR (KBr) 2170, 1980, 1620 cm^{-1}; ^1H NMR ($CDCl_3$) δ 5.39 (s, 10 H, 2 × C_5H_5), 3.96 (sept, 1 H, J = 8 Hz, C*H*), 1.35 (d, 6 H, J = 8 Hz, 2 × CH_3); ^{19}F NMR ($CDCl_3$) δ −54.9 (s); MS, m/z (relative intensity) 595 $[M]^+$ (1), 567 $[M - CO]^+$ (17), 548 $[M - CO - F]^+$ (2), 526 $[M - CN\text{-}i\text{-}Pr]^+$ (4), 233 $[C_{10}H_{10}Rh]^+$ (100).

CyNC. The reaction between **1** (0.082 g) and cyclohexyl isocyanide gave a major orange product and a minor orange-red product. Attempts to obtain an analytically pure sample of the major product by pouring a fresh reaction solution into pentane were not successful. Spectral data established that the major product is $(\eta\text{-}C_5H_5)_2Rh_2(CO)(CNCy)(\mu\text{-}CF_3C_2CF_3)$ (0.090 g, 90%). Spectroscopic data: IR (CH_2Cl_2) ν(CN) at 2140 vs, ν(CO) at 1980 vs, ν(C=C) at 1635 m cm^{-1}; ^1H NMR ($CDCl_3$) δ 5.40 (s, 10 H, 2 × C_5H_5), 3.7 and 1.9–1.2 (2 × m, 11 H, Cy); ^{19}F NMR ($CDCl_3$) δ −54.8 (s); MS, m/z (relative intensity) 607 $[M]^+$ (6), 588 $[M - F]^+$ (1), 233 $[C_{10}H_{10}Rh]^+$ (100).

2,6-$Me_2C_6H_3NC$. The reaction between **1** (0.080 g) and 2,6-dimethylphenyl isocyanide gave a minor orange compound, which was not identified, and a major product. The latter was isolated as orange crystals of $(\eta\text{-}C_5H_5)_2Rh_2(CO)(CNC_6H_3Me_2)(\mu\text{-}CF_3C_2CF_3)$ (0.097 g, 97%), mp >250 °C. Anal. Calcd for $C_{23}H_{19}F_6NORh_2$: C, 42.8; H, 3.0; F, 17.7; N, 2.2. Found: C, 43.1; H, 3.1; F, 17.7; N, 1.9. Spectroscopic data: IR (CH_2Cl_2) ν(CN) at 2135 vs, ν(CO) at 1985 vs, ν(C=C) at 1630 m cm^{-1}; ^1H NMR (acetone-d_6) δ 7.19 (s, 3 H, C_6H_3), 5.57 (s, 10 H, 2 × C_5H_5), 2.38 (s, 6 H, 2 × CH_3); ^{19}F NMR (acetone-d_6) δ −53.3 (s); MS, m/z (relative intensity) 657 $[M]^+$ (<1), 629 $[M - CO]^+$ (9), 168 $[C_5H_5Rh]^+$ (100). There was no isomerization of $(\eta\text{-}C_5H_5)_2Rh_2(CO)(CNC_6H_3Me_2)(\mu\text{-}CF_3C_2CF_3)$ upon prolonged heating in refluxing dichloromethane.

Reaction of $(\eta\text{-}C_5H_5)_2Rh_2(CO)_2(\mu\text{-}CF_3C_2CF_3)$ with RNCO. R = *p*-MeC_6H_4NCO. A solution of $(\eta\text{-}C_5H_5)_2Rh_2(CO)_2(\mu\text{-}CF_3C_2CF_3)$ (0.031 g) and *p*-tolyl isocyanate (0.042 g, mole ratio = 1:6) in hexane/dichloromethane (15 mL, 2:1 v/v) was heated in an evacuated Carius tube at 120 °C for 24 h. Solvent and excess ligand were removed under reduced pressure to yield a red-purple solid. TLC with a 1:1 mixture of X4/dichloromethane as eluent developed three main bands. The first two gave unchanged starting material (0.012 g, 39%) and the purple solid $(\eta\text{-}C_5H_5)_3Rh_3(\mu\text{-}CO)(\mu\text{-}CF_3C_2CF_3)$[13] (0.003 g, 6%). The final crimson band gave $(\eta\text{-}C_5H_5)_2Rh_2\{\mu\text{-}\eta^3\text{-}N(C_6H_4Me\text{-}p)C(O)C(CF_3)C(CF_3)\}$[6] (0.010 g, 27%). All products were characterized spectroscopically.

Repetition of the reaction $[(\eta\text{-}C_5H_5)_2Rh_2(CO)_2(\mu\text{-}CF_3C_2CF_3)$ (0.048 g), *p*-tolyl isocyanate (0.053 g, mole ratio = 1:4.5), and hexane/dichloromethane (19:1 v/v, 20 mL)] at 200 °C for 17 h and subsequent TLC with a 1:1 mixture of X4/dichloromethane separated four bands. The first gave yellow-orange crystals of $(\eta\text{-}C_5H_5)_3Rh_3\{\mu\text{-}C(CF_3)\}_2$ (0.007 g, 12%), mp >250 °C, which was identified spectroscopically. Spectral data: IR (CH_2Cl_2) 1280 m, 1250 sh, 1100 vs, 960 s cm^{-1}; ^1H NMR ($CDCl_3$) δ 5.16 (s, C_5H_5); ^{19}F NMR ($CDCl_3$) δ −52.5 (s, 2 × CF_3); MS, m/z (relative intensity) 666 $[M]^+$ (30), 601 $[M - C_5H_5]^+$ (<5), 585 $[M - CCF_3]^+$ (<5), 233 $[C_{10}H_{10}Rh]^+$ (100). The second band gave orange-red crystals of $(\eta\text{-}C_5H_5)_2Rh_2\{C_4(CF_3)_4\}$[14] (0.005 g, 8%). The purple solid $(\eta\text{-}C_5H_5)_3Rh_3(\mu\text{-}CO)(\mu\text{-}CF_3C_2CF_3)$[13] (0.009 g, 21%) was obtained from the third band, and the final crimson band gave $(\eta\text{-}C_5H_5)_2Rh_2\{\mu\text{-}\eta^3\text{-}N(C_6H_4Me\text{-}p)C(O)C(CF_3)C(CF_3)\}$ (0.014 g, 26%).

R = Me. In the same manner, a 1:7 mole ratio of $(\eta\text{-}C_5H_5)_2Rh_2(CO)_2(\mu\text{-}CF_3C_2CF_3)$ (0.034 g) and methyl isocyanate (0.024 g) was heated at 120 °C for 24 h. TLC separated $(\eta\text{-}C_5H_5)_3Rh_3(\mu\text{-}CO)(\mu\text{-}CF_3C_2CF_3)$ (0.012 g, 41%) and minor products from a crimson-red product. The latter was isolated as crimson-red crystals, $(\eta\text{-}C_5H_5)_2Rh_2\{\mu\text{-}\eta^3\text{-}N(Me)C(O)C(CF_3)C(CF_3)\}$[6] (0.007 g, 21%); it was characterized spectroscopically.

Repetition of the reaction with a 1:9 mole ratio of $(\eta\text{-}C_5H_5)_2Rh_2(CO)_2(\mu\text{-}CF_3C_2CF_3)$ (0.052 g) and methyl isocyanate (0.048 g) at 200 °C for 17 h, and subsequent TLC, gave four products. These were identified spectroscopically as $(\eta\text{-}C_5H_5)_3Rh_3\{\mu\text{-}C(CF_3)\}_2$ (0.007 g, 11%), $(\eta\text{-}C_5H_5)_2Rh_2\{C_4(CF_3)_4\}$ (0.003 g, 5%), $(\eta\text{-}C_5H_5)_3Rh_3(\mu\text{-}CO)(\mu\text{-}CF_3C_2CF_3)$ (0.009 g, 21%), and $(\eta\text{-}C_5H_5)_2Rh_2\{\mu\text{-}\eta^3\text{-}N(Me)C(O)C(CF_3)C(CF_3)\}$ (0.013 g, 25%).

R = *t*-Bu. At 120 °C for 24 h, a 1:4 mole ratio of $(\eta\text{-}C_5H_5)_2Rh_2(CO)_2(\mu\text{-}CF_3C_2CF_3)$ (0.052 g) and *tert*-butyl isocyanate (0.035 g) gave unchanged starting complex (0.031 g, 59%) and $(\eta\text{-}C_5H_5)_3Rh_3(\mu\text{-}CO)(\mu\text{-}CF_3C_2CF_3)$ (0.004 g, 9%).

At 200 °C for 17 h, a 1:3 mole ratio of $(\eta\text{-}C_5H_5)_2Rh_2(CO)_2(\mu\text{-}CF_3C_2CF_3)$ (0.048 g) and *tert*-butyl isocyanate (0.022 g) gave $(\eta\text{-}C_5H_5)_3Rh_3\{\mu\text{-}C(CF_3)\}_2$ (0.007 g, 12%), $(\eta\text{-}C_5H_5)_2Rh_2\{C_4(CF_3)_4\}$ (0.010 g, 17%), $(\eta\text{-}C_5H_5)_3Rh_3(\mu\text{-}CO)(\mu\text{-}CF_3C_2CF_3)$ (0.011 g, 28%), and $(\eta\text{-}C_5H_5)_2Rh_2\{\mu\text{-}\eta^3\text{-}N(t\text{-}Bu)C(O)C(CF_3)C(CF_3)\}$[6] (0.012 g, 23%).

Oxidation of $(\eta\text{-}C_5H_5)_2Rh_2(CO)(CNR)(\mu\text{-}CF_3C_2CF_3)$ with Me_3NO. A typical procedure for the reaction of $(\eta\text{-}C_5H_5)_2Rh_2(CO)(CNR)(\mu\text{-}CF_3C_2CF_3)$ with anhydrous Me_3NO is given below for the system with R = *p*-$MeOC_6H_4$.

$(\eta\text{-}C_5H_5)_2Rh_2(CO)(CNC_6H_4OMe\text{-}p)(\mu\text{-}CF_3C_2CF_3)$ (as the rearranged isomer)[7] (0.052 g) and trimethylamine *N*-oxide (0.010 g, mole ratio = 1:2) were kept in refluxing acetone for 30 min. CO_2 was detected by passing gaseous products through a trap containing aqueous barium hydroxide. TLC of the reaction solution with 10:2 CH_2Cl_2/Et_2O as eluent separated numerous trace bands from a major crimson band. The latter gave crimson crystals of $(\eta\text{-}C_5H_5)_2Rh_2\{\mu\text{-}\eta^3\text{-}N(C_6H_4OMe\text{-}p)C(O)C(CF_3)C(CF_3)\}$ (0.045 g, 88%), mp 257–259 °C. Anal. Calcd for $C_{22}H_{17}F_6NO_2Rh_2$: C, 40.8;

(9) Amarego, W. L. F.; Perrin, D. D.; Perrin, D. R. *Purification of Laboratory Chemicals*, 2nd ed.; Pergamon: Oxford, 1980.
(10) Dickson, R. S.; Gatehouse, B. M.; Nesbit, M. C.; Pain, G. N. *J. Organomet. Chem.* **1981**, *215*, 97.
(11) Weber, W. P.; Gokel, G. W.; Ugi, I. K. *Angew. Chem., Int. Ed. Engl.* **1972**, *11*, 530.
(12) Weber, W. P.; Gokel, G. W. *Tetrahedron Lett.* **1972**, 1637.
(13) Dickson, R. S.; Mok, C.; Pain, G. N. *J. Organomet. Chem.* **1979**, *166*, 385.
(14) Corrigan, P. A.; Dickson, R. S.; Johnson, S. H.; Pain, G. N.; Yeoh, M. *Aust. J. Chem.* **1982**, *35*, 2203.

H, 2.7; F, 17.6; N, 2.2. Found: C, 41.1; H, 2.7; F, 17.8; N, 1.9. Spectroscopic data: IR (CH_2Cl_2) ν(CO) at 1720 and 1700 vs cm^{-1}; ^1H NMR (acetone-d_6) δ 6.87 ± 0.16 (m, AA'XX' system, 4 H, C_6H_4), 5.88 (d, 5 H, J = 0.9 Hz, C_5H_5), 5.19 (s, 5 H, C_5H_5), 3.75 (s, 3 H, OCH_3); ^{19}F NMR (acetone-d_6) δ −48.4 (q, 3 F, J = 13 Hz, CF_3), −57.5 (q, 3 F, J = 13 Hz, CF_3); MS, m/z (relative intensity) 647 $[M]^+$ (52), 498 $[M - OCNR]^+$ (24), 233 $[C_{10}H_{10}Rh]^+$ (100).

The following new compounds were obtained in similar manner. **(η-C_5H_5)$_2$Rh$_2$(μ-η^3-N(C_2H_5)C(O)C(CF_3)C(CF_3)}**: crimson crystals (17% after 4 h); mp 257 °C. Anal. Calcd for $C_{17}H_{15}F_6NO_2Rh_2$: C, 35.9; H 2.7; F, 20.0; N, 2.5. Found: C, 36.4; H, 2.7; F, 19.8; N, 2.3. Spectroscopic data: IR (CH_2Cl_2) ν(CO) at 1675 sh, 1660 vs cm^{-1}; ^1H NMR ($CDCl_3$) δ 5.57 (d, 5 H, J = 0.9 Hz, C_5H_5), 5.30 (s, 5 H, C_5H_5), 3.07 (m, 2 H, CHH'), 1.15 (dd, 3 H, $J \approx J' \approx 7$ Hz, CH_3); ^{19}F NMR ($CDCl_3$) δ −48.5 (q, 3 F, J = 12 Hz, CF_3), −57.4 (q, 3 F, J = 12 Hz, CF_3); MS, m/z (relative intensity) 569 $[M]^+$ (6), 553 $[M - O]^+$ (4), 498 $[M - OCNR]^+$ (4), 233 $[C_{10}H_{10}Rh]^+$ (100).

(η-C_5H_5)$_2$Rh$_2$(μ-η^3-N($C_6H_3Me_2$-2,6)C(O)C(CF_3)C(CF_3)}: brown crystals (26% after 3 h); mp 196 °C. Anal. Calcd for $C_{24}H_{19}F_6NORh_2$: C, 43.9; H, 2.9; F, 17.4; N, 2.1. Found: C, 43.8; H, 2.9; F, 17.5; N, 2.1. Spectroscopic data: IR (CH_2Cl_2) ν(CO) at 1650 vs cm^{-1}; ^1H NMR (acetone-d_6) δ 6.89 (s, 3 H, C_6H_3), 5.86 (d, 5 H, J = 0.9 Hz, C_5H_5), 5.07 (s, 5 H, C_5H_5), 2.37 (s, 6 H, 2 × CH_3); ^{19}F NMR (acetone-d_6) δ −46.1 (q, 3 F, J = 12 Hz, CF_3), −56.4 (q, 3 F, J = 12 Hz, CF_3); MS, m/z (relative intensity) 645 $[M]^+$ (10), 626 $[M - F]^+$ (<1), 498 $[M - OCNR]^+$ (20), 233 $[C_{10}H_{10}Rh]^+$ (100).

(η-C_5H_5)$_2$Rh$_2$(μ-η^3-N($C_6H_4NO_2$-*p*)C(O)C(CF_3)C(CF_3)}:[7] crimson crystals (47% after 3 h); mp >250 °C. Anal. Calcd for $C_{21}H_{14}F_6N_2O_3Rh_2$: C, 38.1; H, 2.1; F, 17.2; N, 4.2. Found: C, 38.4; H, 2.1; F, 16.9; N, 4.1. Spectroscopic data: IR (CH_2Cl_2) ν(CO) at 1710 sh, 1690 vs (br) cm^{-1}; ^1H NMR ($CDCl_3$) δ 8.04 (dm, 2 H, J = 9 Hz, C_6H_2), 7.23 (dm, 2 H, J = 9 Hz, C_6H_2), 5.73 (d, 5 H, J = 0.7 Hz, C_5H_5), 5.05 (s, 5 H, C_5H_5); ^{19}F NMR ($CDCl_3$) δ −48.6 (q, 3 F, J = 13 Hz, CF_3), −57.6 (q, 3 F, J = 13 Hz, CF_3); MS, m/z (relative intensity) 662 $[M]^+$ (10), 632 $[M - NO]^+$ (4), 233 $[C_{10}H_{10}Rh]^+$ (100).

Preparation of the known[6] compounds (η-C_5H_5)$_2$Rh$_2$(μ-η^3-N(R)C(O)C(CF_3)C(CF_3)}, R = Cy (28% yield after 10 h) and Ph (51% after 3 h), was also achieved in this way.

Procedure for Electrochemistry. Solutions of dirhodium complexes were prepared just prior to use by dissolution in acetonitrile which was 0.1 M in Et_4NClO_4 or in dichloromethane which was 0.1 M in Bu_4NClO_4. Sample solutions were protected from direct exposure to light and were deaerated with prepurified nitrogen or argon. The reference electrode was coupled to the electrochemical cell through a porous Vycor bridge that contained the same supporting electrolyte and solvent as was in the cell. In each case, the same electrochemical experiment was also performed on the same concentration of ferrocene during the same work period, and all voltages were referenced to the reversible $E^r_{1/2}$ value (approximately E°) for the ferrocene–ferricinium couple (Fc/Fc^+). The temperature used for measurements was (20 ± 1) °C unless otherwise stated.

Crystallography. Well-formed single crystals of (η-C_5H_5)$_2$Rh$_2$(CO)($CNC_6H_3Me_2$-2,6)(μ-$CF_3C_2CF_3$) were grown from chloroform. A representative transparent red tabular crystal was used for data collection. Intensity measurements were made on a Philips PW1100 diffractometer with graphite monochromated Mo Kα radiation at 295 K. Cell parameters were determined from 24 accurately centered reflections and were calculated by the standard Philips program. Other crystal data are summarized in Table I. Three standard reflections monitored every 4 h showed no significant variation in intensity over the data collection period.

Intensity data were processed as described previously.[15] A numerical absorption correction was applied, the maximum and minimum transmission factors being 0.912 and 0.743, respectively. The atomic scattering factors for neutral atoms were taken from ref 16 and were corrected for anomalous dispersion by using values from ref 16. All calculations were performed on a VAX 11/780 computer. The program used for least-squares refinement was that due to Sheldrick.[17] Hydrogen atoms were not included in the calculations.

The structure was solved by conventional Patterson and Fourier techniques. The locations of all non-hydrogen atoms were refined by full-matrix least-squares methods employing anisotropic thermal parameters for Rh and F and isotropic thermal parameters for all other atoms. Final positional parameters are given in Table II and bond lengths and angles in Table III, and Figure 1 shows the atomic labeling scheme used. Material deposited

Table I. Summary of Crystal Structure Data for the Complex (η-C_5H_5)$_2$Rh$_2$(CO)($CNC_6H_3Me_2$)($CF_3C_2CF_3$)

(a) Crystal Data	
formula	$C_{24}H_{19}F_6NORh_2$
mol wt	657.9
cryst system	orthorhombic
space system	*Pbca*
a, Å	17.950 (8)
b, Å	17.161 (8)
c, Å	15.273 (7)
U, Å^3	4704.7
Z	8
D(calcd), g cm^{-3}	1.86
D(measd), g cm^{-3}	1.84 (2)
F(000)	2576
μ(Mo Kα), cm^{-1}	14.4
(b) Data Collection	
cryst dimens, mm	0.06 × 0.30 × 0.25
2θ limis, deg	6–60
ω scan angle, deg	±(0.70 + 0.3 tan θ)
scan rate, deg s^{-1}	0.06
total data	6862
data $I > 3\sigma(I)$	2306
final R and R_w	0.061 and 0.057
weight w	$[\sigma^2(F_o)]^{-1}$

Table II. Non-Hydrogen Atom Coordinates

atom	x	y	z
Rh(1)	0.53717 (6)	0.13237 (6)	0.35425 (7)
Rh(2)	0.43025 (6)	0.08918 (6)	0.24245 (7)
F(1)	0.6878 (5)	0.0011 (6)	0.2855 (8)
F(2)	0.6263 (6)	−0.0942 (5)	0.3326 (9)
F(3)	0.6527 (7)	−0.0034 (8)	0.4132 (7)
F(4)	0.5699 (7)	−0.0909 (7)	0.1629 (9)
F(5)	0.4889 (7)	−0.1311 (5)	0.2414 (9)
F(6)	0.4577 (9)	−0.0684 (6)	0.1371 (10)
N(1)	0.6355 (6)	0.1840 (6)	0.2032 (8)
O(1)	0.3530 (7)	0.0074 (7)	0.3882 (7)
C(1)	0.6306 (9)	−0.0187 (10)	0.3336 (12)
C(2)	0.5599 (6)	0.0229 (7)	0.3066 (8)
C(3)	0.5107 (7)	0.0047 (7)	0.2499 (10)
C(4)	0.5059 (1)	−0.0675 (10)	0.1976 (12)
C(5)	0.3855 (8)	0.0408 (8)	0.3346 (9)
C(6)	0.5961 (7)	0.1648 (7)	0.2570 (10)
C(7)	0.6883 (7)	0.2054 (7)	0.1388 (10)
C(8)	0.7217 (8)	0.2796 (9)	0.1507 (11)
C(9)	0.7752 (10)	0.2981 (10)	0.0810 (13)
C(10)	0.7857 (10)	0.2508 (13)	0.0158 (13)
C(11)	0.7540 (11)	0.1791 (11)	0.0051 (12)
C(12)	0.7003 (10)	0.1544 (10)	0.0684 (12)
C(13)	0.7047 (10)	0.3289 (11)	0.2258 (13)
C(14)	0.6609 (10)	0.0758 (10)	0.0623 (12)
C(15)	0.5902 (10)	0.1614 (10)	0.4827 (11)
C(16)	0.5624 (9)	0.2312 (10)	0.4427 (11)
C(17)	0.4848 (8)	0.2277 (9)	0.4353 (10)
C(18)	0.4628 (9)	0.1537 (8)	0.4730 (10)
C(19)	0.5260 (9)	0.1139 (9)	0.5011 (10)
C(20)	0.3301 (9)	0.1486 (9)	0.1838 (11)
C(21)	0.3563 (10)	0.0945 (10)	0.1248 (11)
C(22)	0.4304 (11)	0.1185 (11)	0.0990 (12)
C(23)	0.4454 (10)	0.1883 (10)	0.1492 (13)
C(24)	0.3851 (10)	0.2060 (10)	0.1983 (12)

(15) Fallon, G. D.; Gatehouse, B. M. *J. Solid State Chem.* **1980**, *34*, 193.

(16) Ibers, J. A., Hamilton, W. C., Eds. *International Tables for X-ray Crystallography*; Kynoch: Birmingham, 1974; Vol. 4.

(17) Sheldrick, G. M. SHELX-76 Program for Crystal Structure Determination, Cambridge, England, 1975.

Table III. Some Important Bond Lengths (Å) and Angles (deg) for $(\eta\text{-}C_5H_5)_2Rh_2(CO)(CNC_6H_3Me_2\text{-}2,6)(\mu\text{-}CF_3C_2CF_3)$

(a) Bond Lengths

Rh(1)–Rh(2)	2.674 (2)	Rh(2)–C(5)	1.82 (1)
Rh(1)–C(2)	2.06 (1)	C(2)–C(3)	1.28 (2)
Rh(1)–C(6)	1.91 (1)	C(5)–O(1)	1.16 (2)
Rh(2)–C(3)	2.05 (1)	C(6)–N(1)	1.13 (2)

(b) Bond Angles

Rh(2)–Rh(1)–C(6)	89.0 (4)	C(1)–C(2)–C(3)	130.6 (12)
Rh(2)–Rh(1)–C(2)	70.3 (3)	C(2)–C(3)–C(4)	127.7 (13)
Rh(1)–Rh(2)–C(5)	87.1 (4)	Rh(2)–C(3)–C(2)	110.7 (9)
Rh(1)–Rh(2)–C(3)	69.8 (4)	Rh(2)–C(3)–C(4)	121.5 (11)
Rh(1)–C(2)–C(1)	120.1 (9)	Rh(2)–C(5)–O(1)	174.3 (13)
Rh(1)–C(2)–C(3)	109.0 (9)	Rh(1)–C(6)–N(1)	175.0 (13)

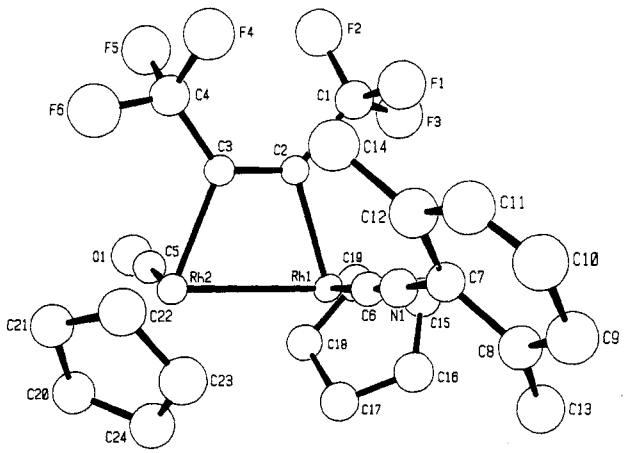

Figure 1. Molecular structure of the complex $(\eta\text{-}C_5H_5)_2Rh_2(CO)(CNC_6H_3Me_2\text{-}2,6)(\mu\text{-}CF_3C_2CF_3)$.

comprises structure factor amplitudes, thermal parameters, and ligand geometries.

Results and Discussion

The Addition of RNC to $(\eta\text{-}C_5H_5)_2Rh_2(\mu\text{-}CO)(\mu\text{-}CF_3C_2CF_3)$. When the isocyanides RNC (R = Et, *i*-Pr, Cy, 2,6-$Me_2C_6H_3$) are added to solutions of $(\eta\text{-}C_5H_5)_2Rh_2(\mu\text{-}CO)(\mu\text{-}CF_3C_2CF_3)$ (**1**), there is an immediate color change from green to orange-red. Spectroscopic data indicates that the addition products $(\eta\text{-}C_5H_5)_2Rh_2(CO)(CNR)(\mu\text{-}CF_3C_2CF_3)$ (**2**) are formed initially. Each of the complexes **2** (R = Et, *i*-Pr, 2,6-$Me_2C_6H_3$) has been obtained analytically pure. Essentially quantitative yields of the compounds are isolated if the reaction solutions are chromatographed immediately after adding the isocyanide to **1**. A better technique is to pour the reaction mixture into hexane which causes the precipitation of orange crystals of the product. It was not possible to isolate pure samples of **2**, R = Cy, by either technique, but full spectroscopic characterization of this compound was achieved.

In the infrared spectra of **2**, $\nu(C{\equiv}N)$ and $\nu(C{\equiv}O)$ are observed within the ranges 2170–2135 and 1990–1980 cm^{-1}, respectively. This is consistent with a structure which incorporates terminal CO and CNR groups, but it does not establish whether these groups have a cis or trans orientation relative to the Rh–Rh bond. X-ray studies described below reveal that the stereochemistry is trans in crystals of the complex; the same geometry was found[13] previously for the more stable of the two geometric isomers of $(\eta\text{-}C_5H_5)_2Rh_2(CO)_2(\mu\text{-}CF_3C_2CF_3)$. Although it seems reasonable to assume that the CO and CNR groups remain trans in solution, there will be further consideration of this point in relation to electrochemical studies described below. The NMR spectra of **2** are simpler than might be expected. Only one C_5H_5 signal is observed in the ^1H spectrum; similarly, just one CF_3 chemical shift is found in the ^{19}F spectrum. The deceptively simple spectra for all complexes are consistent with rapid scrambling of the CO and CNR ligands via a pairwise bridge opening and closing mechanism. This mechanism was elaborated in an earlier variable-temperature NMR study[5] of the complex **2**, R = *t*-Bu.

Scheme I. Possible Pathways for the Reaction between $(\eta\text{-}C_5H_5)_2Rh_2(CO)_2(CF_3C_2CF_3)$ and RNCO

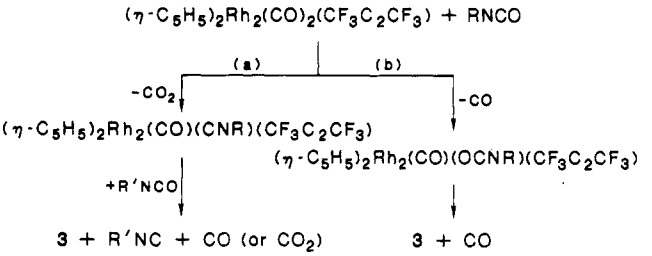

Most of the complexes **2** isomerize to a new species when left in solution. This is not so when R = 2,6-$Me_2C_6H_3$, even when the solutions are refluxed; similar behavior was observed when R = *t*-Bu. Presumably the bulk of these substituents blocks the rearrangement necessary to achieve isomerization.

The Reaction of $(\eta\text{-}C_5H_5)_2Rh_2(CO)_2(\mu\text{-}CF_3C_2CF_3)$ with RNCO. The formation of **2** from **1** and CNR is a straightforward coordinative addition reaction. Investigation of an alternative possible synthesis of the complexes **2** was prompted by the known reaction[18] shown in eq 1. Given that a bound CO in $(\eta\text{-}C_5H_5)_2Rh_2(CO)_2(\mu\text{-}CF_3C_2CF_3)$ is readily oxidized by Me_3NO (eq 2),[5] it seemed reasonable to expect the similar reaction shown in eq 3 to proceed.

$$Fe(CO)_5 + RNCO \rightarrow Fe(CO)_4(CNR) + CO_2 \quad (1)$$

$$(\eta\text{-}C_5H_5)_2Rh_2(CO)_2(\mu\text{-}CF_3C_2CF_3) + Me_3NO \rightarrow (\eta\text{-}C_5H_5)_2Rh_2(\mu\text{-}CO)(\mu\text{-}CF_3C_2CF_3) + CO_2 + Me_3N \quad (2)$$

$$(\eta\text{-}C_5H_5)_2Rh_2(CO)_2(\mu\text{-}CF_3C_2CF_3) + RNCO \rightarrow (\eta\text{-}C_5H_5)_2Rh_2(CO)(CNR)(\mu\text{-}CF_3C_2CF_3) + CO_2 \quad (3)$$

Reactions were attempted with RNCO (R = Me, *t*-Bu, *p*-MeC_6H_4). Although no reaction was observed below 70 °C, a reaction did occur for R = Me and *p*-MeC_6H_4 (but not *t*-Bu) after prolonged heating at 120 °C. However, the product expected according to eq 3 was not obtained. Instead, the major product was the bridging acrylamide complex $(\eta\text{-}C_5H_5)_2Rh_2\{\mu\text{-}\eta^3\text{-}N(R)C(O)C(CF_3)C(CF_3)\}$ (**3**). At 200 °C, the same product was obtained in yields of 25–45% for all systems including R = *t*-Bu. Gaseous products from the reactions were vented through aqueous barium hydroxide solution to detect any CO_2. The amount varied according to R = Me > *t*-Bu > *p*-MeC_6H_4. Two reasonable pathways are shown in Scheme I, and it seems that pathway a is favored when R = Me, but pathway b predominates when R = *p*-MeC_6H_4.

In path b, thermally initiated substitution of CO by OCNR is followed by further loss of CO with formation of **3**; no CO_2 is evolved. The second step in the reaction sequence is analogous to known reactions[6] between **1** and RNCO which occur slowly at 70–80 °C for R = Me, *t*-Bu, and *p*-MeC_6H_4.

Path a is initiated by oxidation of a CO ligand with OCNR. The transfer of O from OCNR gives CO_2 and **1** which captures the coproduct CNR to form **2**. A second OCNR is required to complete this reaction; it oxidizes the bound CNR ligand to OCNR which condenses with the hexafluorobutyne. In this oxidation step, it is possible that

(18) Ulrich, H.; Tucker, B.; Sayigh, A. A. R. *Tetrahedron Lett.* **1967**, 1731.

Table IV. Summary of Electrochemical Reduction Data for $(\eta\text{-}C_5H_5)_2Rh_2(CO)L(\mu\text{-}CF_3C_2CF_3)$ Complexes

complex[a]	electrode	solv	$(E_p^{red.})_1$ or $(E_{1/2}^{red.})_1$, V vs Fc/Fc$^+$	$(\Delta E_p)_1$[b] or $(E_{1/4} - E_{3/4})_1$, mV	$(n^{red.})$[c]	$(E_p^{red.})_2$ or $(E_{1/2}^{red.})_2$, V vs Fc/Fc$^+$	comments
4b	stat Pt[d]	CH_2Cl_2	−2.030	160	1	∼−2.3	second peak is on edge of solvent limit
4b	stat Pt[d]	acetone	∼−1.87	∼130	1		process 1 is on edge of solvent limit
4b	stat Pt[d]	CH_3CN	−1.839	100	1	∼−2.2	second peak is drawn out
4b	RPDE[e]	CH_2Cl_2	−1.996	82	1	∼−2.3[f]	second wave is on edge of solvent limit
4b	RPDE[e]	CH_3CN	−1.795	52	1	∼−2.1[f]	second wave is on edge of solvent limit
4b	DME[g]	CH_2Cl_2	−1.936	46	2		single two-electron reduction wave if solution bubbled with CO; multiple waves also present at more negative potential in absence of CO
4b	DME[g]	acetone	−1.789	36	2		single two-electron reduction wave if solution bubbled with CO; multiple waves also present at more negative potential in absence of CO
4b	DME[g]	CH_3CN	−1.777	46	2		single two-electron reduction wave if solution bubbled with CO; multiple waves also present at more negative potential in absence of CO
4b	HMDE[d]	CH_2Cl_2	∼−2.000		2		single two-electron reduction wave if solution bubbled with CO; multiple waves also present at more negative potential in absence of CO
4b	HMDE[d]	acetone	−1.84		2		single two-electron reduction wave if solution bubbled with CO; multiple waves also present at more negative potential in absence of CO
4b	HMDE[d]	CH_3CN	−1.814		2		single two-electron reduction wave if solution bubbled with CO; multiple waves also present at more negative potential in absence of CO
4a	stat Pt[d]	CH_2Cl_2	−2.03		1	−2.3	process 2 is much smaller in height than process 1 and is at edge of solvent limit
4a	stat Pt[d]	CH_3CN	−1.84		1	−2.2	process 2 is much smaller in height than process 1 and is at edge of solvent limit
2	stat Pt[d]	CH_2Cl_2	∼−2.4		1		
2	stat Pt[d]	CH_3CN	−2.24		1		
2	DME[g]	CH_2Cl_2	∼−2.2		*h*		at edge of solvent limit
2	DME[g]	CH_3CN	−2.091	50	2		
5	stat Pt[d]	CH_2Cl_2	−2.202		1		
5	stat Pt[d]	mixed[i]	−2.04		1		
5	DME[g]	CH_2Cl_2	−2.077	53	2		
5	HMDE[g]	CH_2Cl_2	−2.085		1–2		

[a] **4b** = *trans*-$(\eta\text{-}C_5H_5)_2Rh_2(CO)_2(\mu\text{-}CF_3C_2CF_3)$; **4a** = *cis*-$(\eta\text{-}C_5H_5)_2Rh_2(CO)_2(CF_3C_2CF_3)$; **2** = $(\eta\text{-}C_5H_5)_2Rh_2(CO)(CN\text{-}t\text{-}Bu)(\mu\text{-}CF_3C_2CF_3)$; **5** = $(\eta\text{-}C_5H_5)_2Rh_2(CO)(PPh_3)(\mu\text{-}CF_3C_2CF_3)$; concn = 0.4 mM; T = 20 C. [b] For 0.4 mM Fc, $(E_p^{ox}) - (E_p^{red.})$ = 110–150 mV at ν = 200 mV/s. [c] Based on comparison with oxidation current seen for $(\eta\text{-}C_5H_5)_2Rh_2(\mu\text{-}CO)(\mu\text{-}t\text{-}BuC_2\text{-}t\text{-}Bu)$.[25] [d] Scan rate = 200 mV/s. [e] Scan rate = 10 mV/s; rotation speed = 25 rps. [f] For these systems, $(E_{1/4} - E_{3/4})_2 > 100$ mV and $(n^{red.})_2 = 1$. [g] Scan rate = 5 mV/s; drop time = 1 s. [h] Multielectron. [i] 1:1 mixture of 0.1 M TBAP in CH_2Cl_2 and 0.1 M TEAP in CH_3CN.

the CNR ligand in **2** is oxidized in preference to the CO ligand. Alternatively, both CO and CNR ligands could be oxidized simultaneously by OCNR. It is difficult to substantiate any specificity by investigating reactions between $(\eta\text{-}C_5H_5)_2Rh_2(CO)(CNR)(CF_3C_2CF_3)$ and R′NCO because of the relatively harsh reaction conditions required and the consequent diversity of competing reactions.

Several other products were isolated from the reaction mixture. The major ones were the binuclear metalladiene complex $(\eta\text{-}C_5H_5)_2Rh_2\{C_4(CF_3)_4\}$ (yields 5–17%) and the trimeric complexes $(\eta\text{-}C_5H_5)_3Rh_3(\mu\text{-}CO)(\mu\text{-}CF_3C_2CF_3)$ (yields 21–28%) and $(\eta\text{-}C_5H_5)_3Rh_3(\mu\text{-}CCF_3)_2$ (yields 11–12%). Although the latter complex has not been reported previously, analogous dialkylidyne compounds $(\eta\text{-}C_5H_5)_3Rh_3(\mu\text{-}CR)_2$ (R = Ph, *p*-MeC_6H_4) are known.[19] In these compounds, individual CR units sit on either side of the $(\eta\text{-}C_5H_5)_3Rh_3$ plane. Each of these species is formed by pyrolysis of $(\eta\text{-}C_5H_5)_2Rh_2(CO)_2(\mu\text{-}CF_3C_2CF_3)$ under the reaction conditions.

Crystal and Molecular Structure of $(\eta\text{-}C_5H_5)_2Rh_2(CO)(CNC_6H_3Me_2\text{-}2,6)(\mu\text{-}CF_3C_2CF_3)$. The most pertinent feature of the structure is the disposition of the ligands CO and CNR. These are mutually trans and the bonds Rh(1)–C(6)–N(1) and Rh(2)–C(5)–O(1) are approximately linear and close to parallel; both bonds tilt slightly toward the hexafluorobutyne ligand (see supplementary Table III). Nonetheless, the best fit planes through [O(1),C(5),Rh(2),Rh(1),C(6),N(1),C(7)] and [C(1),C(2),Rh(1),Rh(2),C(3),C(4)] are close to perpendicular, with the dihedral angle being 96°. The bond distances within the Rh_2–$CF_3C_2CF_3$ and Rh–CO sections of the molecule are very similar to those previously reported[20] for $(\eta\text{-}C_5H_5)_2Rh_2(CO)_2(\mu\text{-}CF_3C_2CF_3)$. In the present structure, the Rh(1)—C(6) distance within the Rh—C≡NR unit is slightly longer than the Rh(2)—C(5) distance in the Rh—C≡O unit, and this is consistent with somewhat more back-donation in the Rh–carbonyl bond compared to the Rh–isocyanide bond. The most interesting feature of the aryl group attached to the isocyanide–nitrogen is the relative shortness of the adjacent bonds C(9)–C(10) and C(10)–C(11) which seems to indicate some localization of π-electron density at this end on the ring. This aryl ring and the carbon atoms of its methyl substituents are coplanar, and the ring is tilted at an angle of 133° with respect to the plane through [O(1),C(5),Rh(2),Rh(1),C(6),N(1)]. The observed Rh–C–N–R parameters are similar to those reported by Cowie et al.[21] for $[Rh_2Cl(CNMe)_2(\mu\text{-}CF_3C_2CF_3)(\mu\text{-}Ph_2PCH_2PPh_2)_2][BF_4]$ except that the Rh–C distance is somewhat shorter in our complex. In Cowie's complex, both isocyanide ligands are attached to the same rhodium atom and consequently they must share any electron density back donated from the metal.

Comparison of the Electrochemical Behavior of the Complexes $(\eta\text{-}C_5H_5)_2Rh_2(CO)L(\mu\text{-}CF_3C_2CF_3)$ (L = CO, CN-*t*-Bu, PPh_3). The use of rhodium compounds in homogeneous catalysis is well-established.[22] With polynuclear rhodium compounds, the mode of coordination of the ligands may have an important influence on the catalytic activity of the complex. Recent papers[5,23] have highlighted the ability of alkynes coordinated to a rhodium–rhodium bond to twist through 90° as ligands are removed or added. Others[24] have established a correlation between the bonding mode of carbonyl ligands on a rhodium–rhodium bond and the activity of the complexes in the catalytic hydrogenation of alkynes and alkenes. The complexes $(\eta\text{-}C_5H_5)_2Rh_2(CO)L(\mu\text{-}CF_3C_2CF_3)$ (L = CO, CNR, PPh_3), together with $(\eta\text{-}C_5H_5)_2Rh_2(\mu\text{-}CO)(\mu\text{-}CF_3C_2CF_3)$, are potentially interesting as model compounds for such catalytic systems. Consequently, we are interested in exploring factors that can affect the bonding and lability

(19) Clauss, A. D.; Shapley, J. R.; Wilker, C. N.; Hoffmann, R. *Organometallics* **1984**, *3*, 619.
(20) Dickson, R. S.; Johnson, S. H.; Kirsch, H. P.; Lloyd, D. J. *Acta Crystallogr., Sect. B: Struct. Crystallogr. Cryst. Chem.* **1977**, *B33*, 2057.
(21) Cowie, M.; Dickson, R. S.; Hames, B. W. *Organometallics* **1984**, *3*, 1879.
(22) Dickson, R. S. *Homogeneous Catalysis with Compounds of Rhodium and Iridium*; D. Reidel: Dordrecht, 1985.
(23) Hoffman, D. M.; Hoffmann, R.; Fisel, C. R. *J. Am. Chem. Soc.* **1982**, *104*, 3858 and references therein.
(24) Sanger, A. R. *Can. J. Chem.* **1982**, *60*, 1363 and references therein.

Table V. Summary of Electrochemical Oxidation Data for $(\eta\text{-}C_5H_5)_2Rh_2(CO)L(\mu\text{-}CF_3C_2CF_3)$ Complexes

complex[a]	electrode	solv	$(E_p^{ox.})_1$ or $(E_{1/2}^{ox.})_1$, V vs Fc/Fc$^+$	$(\Delta E_p)_1$[b] or $(E_{3/4} - E_{1/4})_1$, mV	$(n^{ox.})_1$[c]	comments
4b	stat Pt[d]	CH_2Cl_2	+0.880		2	
4b	stat Pt[d]	acetone	+0.980		2	
4b	stat Pt[d]	CH_3CN	+0.896		2	
4b	RPDE[e]	CH_2Cl_2	+0.821	115	2	
4b	RPDE[e]	CH_3CN	+0.887	103	2	
4b	DME[f]	CH_2Cl_2	+0.290	40	2	no oxidation wave in CH_3CN
4b	HMDE[d]	CH_2Cl_2	+0.290	73	1–2	$(i_p^{ox.})_1/(i_p^{red.})_1 = 1.0$
4a	stat Pt[d]	CH_3CN	+0.700 (0.890)		2	values in parentheses refer to trans isomer **4b** generated at electrode surface—see text
4a	stat Pt[d]	CH_2Cl_2	+0.670 (0.870)		2	
4a	RPDE[e]	CH_3CN	+0.680 (0.890)		2	
2	stat Pt[d]	CH_2Cl_2	+0.483		1–2	reduction peak observed on reverse scan at approximately 0 V; $(i_p^{ox.})$ < for complex **4b**
2	stat Pt[d]	CH_3CN	+0.465		1–2	reduction peak observed on reverse scan at approximately −0.15 V; $(i_p^{ox.})$ < for complex **4b**
2	RPDE[e]	CH_2Cl_2	+0.417	97	1–2	$(i_l^{ox.})$ < for complex **4b**
2	DME[f]	CH_2Cl_2	+0.103	36	1–2	$(i_l^{ox.})$ < for complex **4b**
2	DME[f]	CH_3CN	~+0.08	?	?	process observed as shoulder on solvent limit
5	stat Pt[d]	CH_2Cl_2	+0.317		1	second irreversible oxidation peak at ~+0.94 V; reduction peak on reverse scan at 0.2 V
5	stat Pt[d]	mixed[g]	+0.272		1	reduction peak observed on reverse scan at approximately 0 V
5	DME[f]	CH_2Cl_2	+0.120	30	1	
5	DME[f]	mixed[g]	+0.060	?	?	process observed as shoulder on solvent limit

[a] **4b** = *trans*-$(\eta\text{-}C_5H_5)_2Rh_2(CO)_2(\mu\text{-}CF_3C_2CF_3)$; **4a** = *cis*$(\eta\text{-}C_5H_5)_2Rh_2(CO)_2(CF_3C_2CF_3)$; **2** = $(\eta\text{-}C_5H_5)_2Rh_2(CO)(CN\text{-}t\text{-}Bu)(\mu\text{-}CF_3C_2CF_3)$; **5** = $(\eta\text{-}C_5H_5)_2Rh_2(CO)(PPh_3)(\mu\text{-}CF_3C_2CF_3)$; concn = 0.4 mM; T = 20 °C. [b] For 0.4 mM Fc, $(E_p^{ox.}) - (E_p^{red.})$ = 110–150 mV at ν = 200 mV/s on stat Pt electrode in CH_2Cl_2. [c] Based on comparison with limiting or peak current for $(\eta\text{-}C_5H_5)_2Rh_2(\mu\text{-}CO)(\mu\text{-}t\text{-}BuC_2\text{-}t\text{-}Bu)$[25] where n is known to be 1. [d] Scan rate = 200 mV/s. [e] Scan rate = 10 mV/s; rotation speed = 25 rps. [f] Scan rate = 5 mV/s; drop time = 1 s. [g] 1:1 mixture of CH_2Cl_2 and CH_3CN.

of the alkyne, carbonyl and other ligands in these dirhodium complexes. With this in mind, we have investigated the redox properties of the formally rhodium(II) complexes $(\eta\text{-}C_5H_5)_2Rh_2(CO)L(\mu\text{-}CF_3C_2CF_3)$ via the use of electrochemical techniques. Electrochemical data under a range of conditions are summarized in Tables IV and V. The bridging carbonyl rhodium(I) complex $(\eta\text{-}C_5H_5)_2Rh_2(\mu\text{-}CO)(\mu\text{-}CF_3C_2CF_3)$ has already been shown[25] to undergo reduction and oxidation processes under voltammetric conditions, and comparisons are made with this system.

Reduction of *trans*- and *cis*-$(\eta\text{-}C_5H_5)_2Rh_2(CO)_2(\mu\text{-}CF_3C_2CF_3)$. Two isomers of the neutral complex $(\eta\text{-}C_5H_5)_2Rh_2(CO)_2(\mu\text{-}CF_3C_2CF_3)$ have been isolated; these have a cis (**4a**) or trans (**4b**) orientation of the two carbonyl

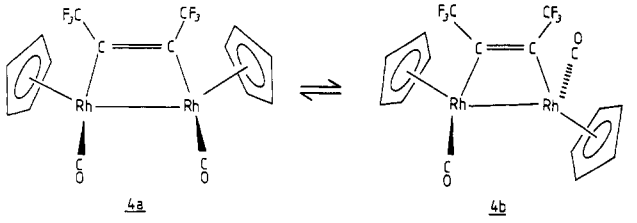

groups. The structure of **4b** has been established[20] from X-ray crystallographic studies and that of **4a** is deduced[10] from spectroscopic results. The cis isomer transforms in solution to the trans form with a half-life at room temperature of about 12 h.[10]

The reduction of $(\eta\text{-}C_5H_5)_2Rh_2(CO)_2(\mu\text{-}CF_3C_2CF_3)$ is remarkably dependent on the isomeric form. Figure 2 shows a rotating platinum disk electrode (RPDE) voltammogram for reduction of the trans isomer **4b** in acetonitrile. Two waves of equal height are observed. The limiting

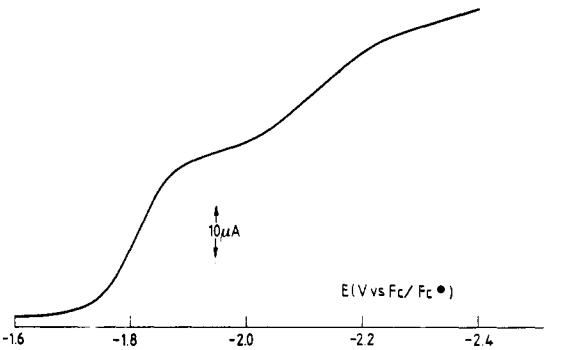

Figure 2. Voltammogram at a rotated platinum disk electrode for reduction of *trans*-$(\eta\text{-}C_5H_5)_2Rh_2(CO)_2(\mu\text{-}CF_3C_2CF_3)$ in 0.1 M Et_4NClO_4 in acetonitrile (scan rate = 10 mV/s; rotation rate = 25 rps; T = 20 °C).

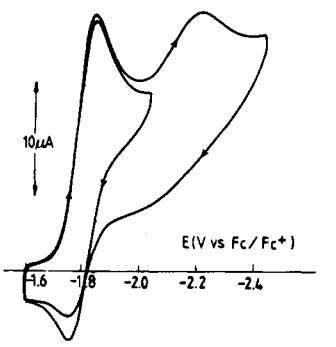

Figure 3. Cyclic voltammogram at a platinum electrode for reduction of *trans*-$(\eta\text{-}C_5H_5)_2Rh_2(CO)_2(\mu\text{-}CF_3C_2CF_3)$ in 0.1 M Et_4NClO_4 in acetonitrile (scan rate = 300 mV/s; T = 20 °C).

current for both processes is linearly dependent on concentration (10^{-4}–10^{-3} M) and the square root of electrode rotation rate, as required for diffusion control. Furthermore, the limiting current per unit concentration (allowing

(25) Bixler, J. W.; Bond, A. M.; Dickson, R. S. *Organometallics* **1986**, *5*, 1435.

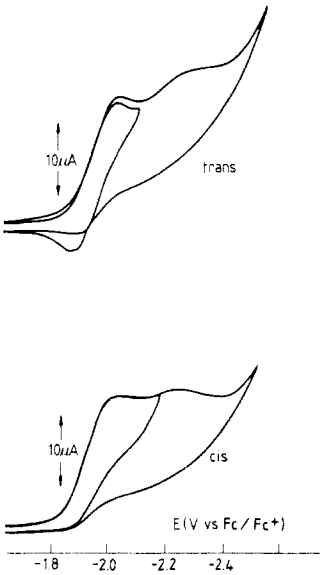

Figure 4. Cyclic voltammograms at a platinum electrode for reduction of *trans*- and *cis*-$(\eta\text{-}C_5H_5)_2Rh_2(CO)_2(\mu\text{-}CF_3C_2CF_3)$ in 0.1 M Bu_4NClO_4 in CH_2Cl_2 (scan rate = 200 mV/s; T = 20 °C).

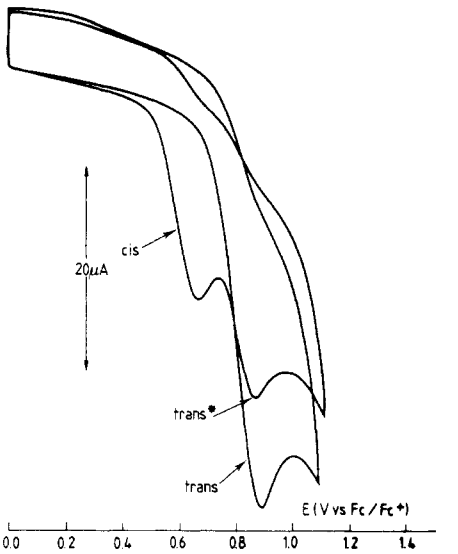

Figure 5. Cyclic voltammograms at a platinum electrode for oxidation of *trans*- and *cis*-$(\eta\text{-}C_5H_5)_2Rh_2(CO)_2(\mu\text{-}CF_3C_2CF_3)$ in 0.1 M Bu_4NClO_4 in dichloromethane (scan rate = 200 mV/s; T = 20 °C); trans* refers to the trans isomer that has been generated at the electrode surface.

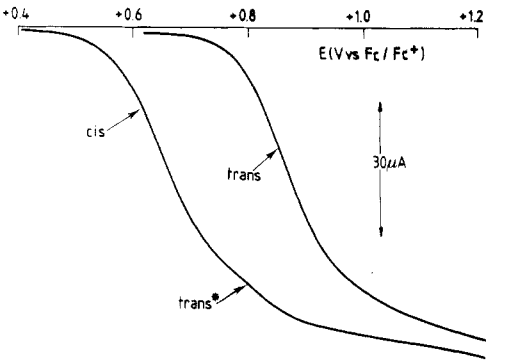

Figure 6. Voltammogram at a rotated platinum disk electrode for oxidation of *cis*- and *trans*-$(\eta\text{-}C_5H_5)_2Rh_2(CO)_2(\mu\text{-}CF_3C_2CF_3)$ in 0.1 M Et_4NClO_4 in acetonitrile (scan rate = 10 mV/s; rotation rate = 25 rps; T = 20 °C); trans* refers to trans isomer that has been generated at the electrode surface.

for sign differences) is identical with that for the known[25] reversible one-electron oxidation of the related complex $(\eta\text{-}C_5H_5)_2Rh_2(\mu\text{-}CO)(\mu\text{-}t\text{-}BuC_2\text{-}t\text{-}Bu)$. These data define both reduction processes as being one-electron processes.

A cyclic voltammogram of **4b** in acetonitrile is shown in Figure 3. This demonstrates that if the potential is switched immediately after the first reduction process, a substantial degree of chemical reversibility exists for this process. However, the first reduction process is not fully reversible in that the peak height for oxidation is always less than that for reduction. The degree of chemical irreversibility is essentially independent of scan rate (50–500 mV s^{-1}) and temperature (+20 to −30 °C). The second reduction process is completely irreversible in the chemical sense and smaller in height than the first reduction process under conditions of cycic voltammetry.

Data in dichloromethane for reduction of **4b** are similar to those in acetonitrile, although substantial catalysis of the solvent reduction process is observed leading to relatively poor resolution of the second reduction process (see Figure 4a). Additionally, greater ohmic *ir* drop effects lead to more drawn out curves than is the case in acetonitrile which has lower resistance. A comparison of cyclic voltammograms for reduction of *cis*- and *trans*-$(\eta\text{-}C_5H_5)_2Rh_2(CO)_2(\mu\text{-}CF_3C_2CF_3)$ in dichloromethane is shown in Figure 4. Remarkably, while the reduction potential for the cis isomer is almost the same as that for the trans isomer, the process is completely irreversible in the chemical sense instead of containing a degree of chemical reversibility. Furthermore, the second reduction process is now very small in height relative to the situation for the second reduction step for the trans isomer. Catalysis of the solvent reduction is still observed in the reductive voltammetry of the cis isomer. The limiting current per unit concentration at RPDE for the first reduction process for the cis and trans isomers have similar values. This implies that the first reduction process remains a one-electron step despite the introduction of chemical irreversibility.

The data obtained with the cis complex **4a** enables some aspects of the mechanism for reduction of the trans isomer **4b** to be understood. For the neutral rhodium(II) complexes, the equilibrium position of the reaction **4a** ⇌ **4b** is known to heavily favor the trans form **4b**. Thus, TLC of solutions of **4a** that have been aged for 48 h show the presence of **4b** and only trace amounts of **4a**; TLC analysis of similarly aged solutions of **4b** reveal no **4a**. However, after a one-electron reduction, the reverse order of stability seems to apply with the cis form of the anion being favored over the trans form. It seems, then, that the isomerization reaction shown in eq 4 is relatively fast compared to that in eq 5. Furthermore, the rate of any rearrangement or

$$trans\text{-}[(\eta\text{-}C_5H_5)_2Rh_2(CO)_2(\mu\text{-}CF_3C_2CF_3)]^- \rightleftharpoons cis\text{-}[(\eta\text{-}C_5H_5)_2Rh_2(CO)_2(\mu\text{-}CF_3C_2CF_3)]^- \quad (4)$$

$$cis\text{-}[(\eta\text{-}C_5H_5)_2Rh_2(CO)_2(\mu\text{-}CF_3C_2CF_3)] \rightleftharpoons trans\text{-}[(\eta\text{-}C_5H_5)_2Rh_2(CO)_2(\mu\text{-}CF_3C_2CF_3)] \quad (5)$$

other molecular change for the trans form of the anion must be much slower than that for the cis anion. Thus, the former is stable on the voltammetric time scale and can be further reduced to a formally rhodium(I) complex whereas the cis form has no inherent stability even on the voltammetric time scale. Reduction of the trans isomer **4b** is consistent with the mechanism represented by eq 6 and 7. A related mechanism for reduction of the cis isomer **4a** is outlined in eq 8 (Scheme II). Formation of the postulated transient bridging carbonyl anionic complexes $[(\eta\text{-}C_5H_5)_2Rh_2(\mu\text{-}CO)(\mu\text{-}CF_3C_2CF_3)]^{2-}$ cannot be proved. However, reductive elimination of CO or related mecha-

Scheme II

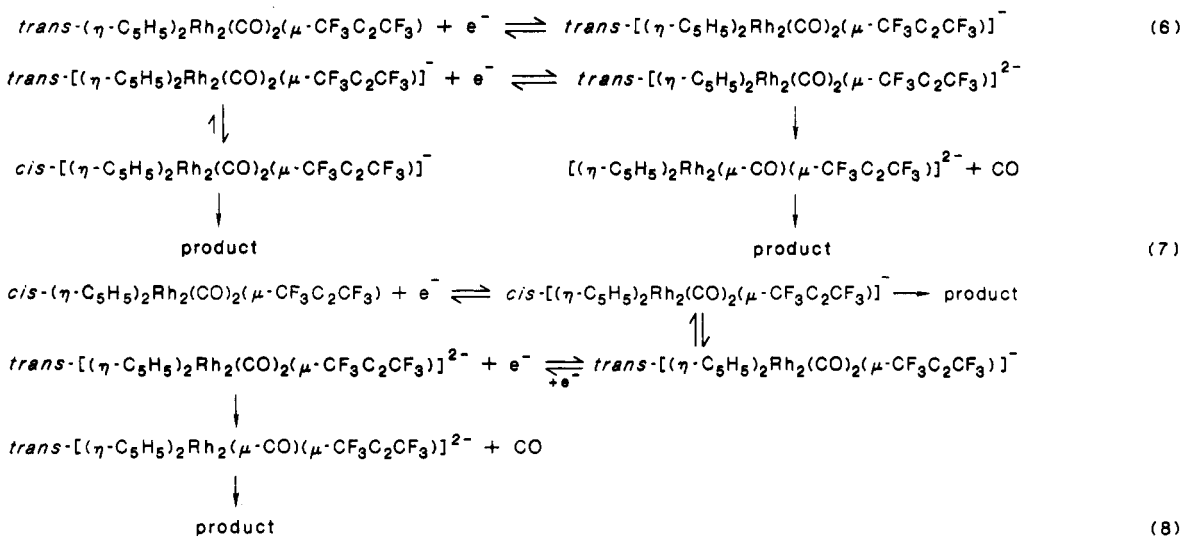

nisms seem plausible given that species such as $(\eta\text{-}C_5H_5)_2Rh_2(\mu\text{-}CO)(\mu\text{-}CF_3C_2CF_3)$ and $[(\eta\text{-}C_5H_5)_2Rh_2(\mu\text{-}CO)(\mu\text{-}CF_3C_2CF_3)]^-$ are reduced at potentials less negative than for reduction of $(\eta\text{-}C_5H_5)_2Rh_2(CO)_2(\mu\text{-}CF_3C_2CF_3)$.

Unfortunately, the products of electrochemical reduction are as yet uncharacterized. Holding the potential of the electrode more negative than the reduction potential for the first reduction process leads to rapid poisoning of the electrode surface. Controlled potential electrolysis experiments are therefore not exhaustive nor highly reproducible. The complexity of the reduction process is confirmed by noting that, at a platinum electrode, the shape of the first reduction process for **4b** is altered by the presence of carbon monoxide. Additionally, at mercury electrodes in acetonitrile, a well-defined single two-electron reduction step is observed for **4b** rather than two one-electron processes. This two-electron reduction process is chemically irreversible at mercury electrodes. In dichloromethane at mercury electrodes, the reduction process is extremely complex and gives rise to several processes. Apparently, the mercury electrode participates directly in the electrochemical reduction process, thereby substantially modifying the reaction sequence from that occurring at a platinum electrode. However, in the presence of CO, the complex series of processes is converted into a single two-electron step with similar characteristics to that in acetonitrile. Again, this is thought to be due to the inhibition of reductive carbonyl elimination reactions associated with the electron-transfer step. The data confirm that the reduced form of the formally rhodium(II) complex $(\eta\text{-}C_5H_5)_2Rh_2(CO)_2(\mu\text{-}CF_3C_2CF_3)$, like that of the formally rhodium(I) system $(\eta\text{-}C_5H_5)_2Rh_2(\mu\text{-}CO)(\mu\text{-}CF_3C_2CF_3)$, is extremely reactive.

Reduction of $(\eta\text{-}C_5H_5)_2Rh_2(CO)L(\mu\text{-}CF_3C_2CF_3)$ (L = *t*-BuNC, PPh_3). The derivatives $(\eta\text{-}C_5H_5)_2Rh_2(CO)(CN\text{-}t\text{-}Bu)(\mu\text{-}CF_3C_2CF_3)$ and $(\eta\text{-}C_5H_5)_2Rh_2(CO)(PPh_3)(\mu\text{-}CF_3C_2CF_3)$ are both reduced at more negative potentials than the dicarbonyl complex (see Table IV). At a platinum electrode, a chemically irreversible one-electron reduction process is observed which shows behavior analogous to that for *cis*-$(\eta\text{-}C_5H_5)_2Rh_2(CO)_2(\mu\text{-}CF_3C_2CF_3)$. However, the structural results reported earlier for the closely related complex $(\eta\text{-}C_5H_5)_2Rh_2(CO)(CNC_6H_3Me_2\text{-}2,6)(\mu\text{-}CF_3C_2CF_3)$ imply that these are trans and not cis isomers. [Crystals of this complex proved more suitable than those of $(\eta\text{-}C_5H_5)_2Rh_2(CO)(CN\text{-}t\text{-}Bu)(\mu\text{-}CF_3C_2CF_3)$ for X-ray crystallographic analysis. However, an incomplete determination of the crystal structure of the CN-*t*-Bu complex established that it has the same structural features as those reported for the $CNC_6H_3Me_2$-2,6 system.] This apparent predicament can be understood if it is assumed that, following electron transfer, isomerization of *trans*-$[(\eta\text{-}C_5H_5)_2Rh_2(CO)L(\mu\text{-}CF_3C_2CF_3)]^-$ to the cis anionic species occurs far more rapidly than was the case with the dicarbonyl complex **4**. This would explain the observation of a chemically irreversible one-electron reduction process rather than a reversible process. The mechanism shown in eq 9 is postulated for reduction of the complexes $(\eta\text{-}C_5H_5)_2Rh_2(CO)L(\mu\text{-}CF_3C_2CF_3)$ at platinum electrodes. The two-electron reduction seen at mercury electrodes (Table V) also parallels the case for the dicarbonyl complex, and direct participation of this electrode material in the reduction process is again indicated.

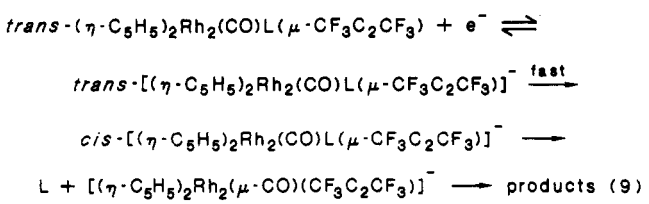

Oxidation of *trans*- and *cis*-$(\eta\text{-}C_5H_5)_2Rh_2(CO)_2(\mu\text{-}CF_3C_2CF_3)$. The oxidation behavior of *trans*- and *cis*-$(\eta\text{-}C_5H_5)_2Rh_2(CO)_2(\mu\text{-}CF_3C_2CF_3)$, as is the case for reduction, is dependent on the isomeric form (see data in Figures 5 and 6 and Table V). However, in this case, the oxidation potentials are well-separated, whereas in the case of reduction they are essentially the same. At a RPDE, a well-defined, chemically irreversible two-electron oxidation process is observed for the trans isomer. The limiting current per unit concentration is twice that for the reversible one-electron oxidation of $(\eta\text{-}C_5H_5)_2Rh_2(\mu\text{-}CO)(\mu\text{-}CF_3C_2CF_3)$[25] and, after allowing for sign differences, also twice that for each of the two one-electron reduction processes detailed previously for *trans*-$(\eta\text{-}C_5H_5)_2Rh_2(CO)_2(\mu\text{-}CF_3C_2CF_3)$.

The oxidation of *cis*-$(\eta\text{-}C_5H_5)_2Rh_2(CO)_2(\mu\text{-}CF_3C_2CF_3)$ occurs in two stages (Figures 5 and 6). The more positive oxidation process is coincident with that for the trans isomer. However, the first step occurs at considerably less positive potential than for oxidation of the trans isomer. The limiting current at a RPDE for the sum of the two oxidation processes is identical with that for the two-electron oxidation of the trans isomer, although the ratio

of the two processes observed with the cis isomer is solvent-dependent (compare Figures 5 and 6).

The overall two-electron oxidation process for both the trans and cis isomers corresponds to oxidation of the formally rhodium(II) complexes to the well-known and highly stable rhodium(III) oxidation state via an ECE mechanism. In the case of oxidation of *cis*-(η-$C_5H_5)_2Rh_2(CO)_2(\mu$-$CF_3C_2CF_3$), the existence of a second process at more positive potential is noted. This corresponds to generation of the trans complex at the electrode surface in significantly higher concentration than is present in the bulk solution and can be explained if it is assumed that isomerization is one reaction pathway which occurs after the initial one-electron transfer process (see eq 10 and 11). The trans cation generated by this isomerization

$$cis\text{-}(\eta\text{-}C_5H_5)_2Rh_2(CO)_2(\mu\text{-}CF_3C_2CF_3) \rightleftharpoons \text{products}$$

$$\uparrow$$

$$cis\text{-}[(\eta\text{-}C_5H_5)_2Rh_2(CO)_2(\mu\text{-}CF_3C_2CF_3)]^+ + e^- \xrightarrow{\text{fast}} trans\text{-}[(\eta\text{-}C_5H_5)_2Rh_2(CO)_2(\mu\text{-}CF_3C_2CF_3)]^+ \quad (10)$$

$$trans\text{-}[(\eta\text{-}C_5H_5)_2Rh_2(CO)_2(\mu\text{-}CF_3C_2CF_3)]^+ + e^- \rightleftharpoons trans\text{-}[(\eta\text{-}C_5H_5)_2Rh_2(CO)_2(\mu\text{-}CF_3C_2CF_3)] \quad (11)$$

pathway would immediately be reduced at a diffusion-controlled rate to *trans*-(η-$C_5H_5)_2Rh_2(CO)_2(\mu$-$CF_3C_2CF_3$), if the $E°$ value for the reaction

$$\text{trans}^+ + e^- \rightleftharpoons \text{trans}^0 \quad (12)$$

occurs at a more positive potential than for the process

$$\text{cis}^+ + e^- \rightleftharpoons \text{cis}^0 \quad (13)$$

The available data indicate that this is the case. The trans^0 complex generated at the electrode surface is then available for oxidation via an ECE mechanism at the same potential as is the case when the trans^0 isomer is present in the bulk solution.

Competitive with the isomerization of the cis$^+$ complex is an ECE mechanism giving rise to a two-electron process. Clearly, neither the trans or cis cationic complexes are inherently stable. Solvent or electrolyte attack followed by elimination of CO to give [(η-$C_5H_5)_2Rh_2(CO)(X)(\mu$-$CF_3C_2CF_3)]^+$ (X = solvent or electrolyte), or elimination of CO to give [(η-$C_5H_5)_2Rh_2(\mu$-CO)(μ-$CF_3C_2CF_3)]^+$, could be expected to lead to an ECE mechanism as the species are more readily oxidized than either *cis*- or *trans*-[(η-$C_5H_5)_2Rh_2(CO)_2(\mu$-$CF_3C_2CF_3)]^+$.

Oxidation of (η-$C_5H_5)_2Rh_2(CO)L(\mu$-$CF_3C_2CF_3$) (L = *t*-BuNC or PPh_3). Substitution of CO by *t*-BuNC or PPh_3 makes the complexes easier to oxidize than the parent dicarbonyl compound (η-$C_5H_5)_2Rh_2(CO)_2(\mu$-$CF_3C_2CF_3$). This is the expected substituent effect. The number of electrons transferred as determined by the limiting current per unit concentration lies in the range of one to two, and well-defined reduction peaks are observed in the reverse scans indicative of formation of solvent dependent products. Data are summarized in Table V. Oxidation processes at mercury electrodes are also observed but occur at very different potentials to the situation at a platinum electrode (see Table V). This implies that interaction of the mercury electrode is involved, as was the case for reduction.

Oxidation of the (η-$C_5H_5)_2Rh_2(CO)L(\mu$-$CF_3C_2CF_3$) derivatives clearly occurs via an initial one-electron process to form a highly reactive cation [(η-$C_5H_5)_2Rh_2(CO)L(\mu$-$CF_3C_2CF_3)]^+$ which can undergo rapid rearrangement. In this case, it can be demonstrated that [(η-$C_5H_5)_2Rh_2(\mu$-CO)(μ-$CF_3C_2CF_3)]^+$ is not a product of rearrangement as no wave corresponding to oxidation of this species is observed. The substituent effect means that (η-$C_5H_5)_2Rh_2(CO)L(\mu$-$CF_3C_2CF_3$) is now oxidized at less positive potential than [(η-$C_5H_5)_2Rh_2(CO)L(\mu$-$CF_3C_2CF_3)]^+$. Consequently, alternative rearrangements are postulated to occur, and the formation of solvent- and substituent-dependent reduction waves in the reverse scan confirms that this is the case.

Chemical Oxidation of the Complexes (η-$C_5H_5)_2Rh_2(CO)(CNR)(\mu$-$CF_3C_2CF_3$). The electrochemical results indicate that it would be difficult to isolate cationic or anionic derivatives formed by oxidation or reduction of the metal atoms in the complexes (η-$C_5H_5)_2Rh_2(CO)(CNR)(\mu$-$CF_3C_2CF_3$). However, oxidation products can be isolated and fully characterized when the complexes are treated with the mild oxidant trimethylamine *N*-oxide, Me_3NO. The products are bridging acrylamide complexes **3** of the same type as are obtained from the reactions of (η-$C_5H_5)_2Rh_2(CO)_2(\mu$-$CF_3C_2CF_3$) with organic isocyanates, RNCO.

These reactions proceed readily in refluxing acetone. The yield of **3** is dependent on R, with the best yield being obtained when R = *p*-$MeOC_6H_4$ (88% after $^1/_2$ h) and the lowest yields when R = 2,6-$Me_2C_6H_3$ (26% after 3 h) or Et (17% after 4 h). In all cases, significant amounts of CO_2 were detected in the gaseous products. These results indicate that both the CO *and* CNR ligands in **2** are susceptible to oxidation under appropriate conditions. It is not easy to rationalize the observed variation in ease of oxidation as R is changed, but it should be noted that **2**, R = *p*-$MeOC_6H_4$, isomerizes extensively in solution whereas **2**, R = 2,6-$Me_2C_6H_3$, does not isomerize at all. Thus, the isomeric form of **2** could be much more susceptible to oxidation than **2** itself.

Conclusions

The bridging carbonyl complex (η-$C_5H_5)_2Rh_2(\mu$-CO)(μ-$CF_3C_2CF_3$) adds a variety of ligands L to form (η-$C_5H_5)_2Rh_2(CO)L(\mu$-$CF_3C_2CF_3$). Isocyanide ligands CNR add coordinatively, but the products are stable to rearrangement only if the R group is bulky. Structural evidence establishes that CNR adds trans to the carbonyl group and that both ligands occupy terminal positions. It has been suggested that the catalytic activity of dirhodium complexes containing terminal carbonyl groups is markedly different from that of related complexes with bridging carbonyls. We find that the redox properties of several complexes (η-$C_5H_5)_2Rh_2(CO)L(\mu$-$CF_3C_2CF_3$) containing a terminal carbonyl are considerably different from those of the bridging carbonyl complex (η-$C_5H_5)_2Rh_2(\mu$-CO)(μ-$CF_3C_2CF_3$). The compounds (η-$C_5H_5)_2Rh_2(CO)L(\mu$-$CF_3C_2CF_3$) (L = CO, *t*-BuNC, PPh_3) are more difficult to reduce and to oxidize than (η-$C_5H_5)_2Rh_2(\mu$-CO)(μ-$CF_3C_2CF_3$). They are also kinetically far more labile on oxidation or reduction. Thus, whereas each member of the series [(η-$C_5H_5)_2Rh_2(\mu$-CO)(μ-$CF_3C_2CF_3)]^{-/0/+/2+}$ has considerable stability on the voltametric time scale, only *trans*-[(η-$C_5H_5)_2Rh_2(CO)_2(\mu$-$CF_3C_2CF_3)]^+$ is observed in the terminal carbonyl series, and it is a very reactive intermediate. The ability of the carbonyl-bridged dirhodium complex to retain its integrity within moderately stable species in different redox states may be connected with the ability of such complexes to act as efficient catalysts in contrast to nonbridged derivatives that undergo extensive rearrangements.

Acknowledgment. This work was assisted by grants from the Australian Research Grants Scheme and the loan of rhodium trichloride from Johnson-Matthey. Technical

assistance from E. MacLennan and D. Luscombe in performing some of the electrochemical experiments is also gratefully acknowledged.

Registry No. 1, 98395-25-6; **4a**, 69881-14-7; **4b**, 63950-13-0; $(\eta\text{-}C_5H_5)_2Rh_2(CO)(CNEt)(\mu\text{-}CF_3C_2CF_3)$, 110294-86-5; $(\eta\text{-}C_5H_5)_2Rh_2(CO)(CN\text{-}i\text{-}Pr)(\mu\text{-}CF_3C_2CF_3)$, 98464-05-2; $(\eta\text{-}C_5H_5)_2Rh_2(CO)(CNCy)(\mu\text{-}CF_3C_2CF_3)$, 98464-04-1; $(\eta\text{-}C_5H_5)_2Rh_2(CO)(CNC_6H_3Me_2)(\mu\text{-}CF_3C_2CF_3$, 110294-85-4; $p\text{-}MeC_6H_4NCO$, 622-58-2; $(\eta\text{-}C_5H_5)_3Rh_3(\mu\text{-}CO)(\mu\text{-}CF_3C_2CF_3)$, 37343-45-6; $(\eta\text{-}C_5H_5)_2Rh_2\{\mu\text{-}\eta^3\text{-}N(C_6H_4Me\text{-}p)C(O)C(CF_3)C(CF_3)\}$, 90883-05-9; $(\eta\text{-}C_5H_5)_3Rh_3\{\mu\text{-}C(CF_3)\}_2$, 110294-87-6; $(\eta\text{-}C_5H_5)_2Rh_2\{C_4(CF_3)_4\}$, 39385-05-2; $(\eta\text{-}C_5H_5)_2Rh_2\{\mu\text{-}\eta^3\text{-}N(Me)C(O)C(CF_3)C(CF_3)\}$, 90860-65-4; $(\eta\text{-}C_5H_5)_2Rh_2\{\mu\text{-}\eta^3\text{-}N(t\text{-}Bu)C(O)C(CF_3)C(CF_3)\}$, 90860-66-5; $(\eta\text{-}C_5H_5)_2Rh_2(CO)(CNC_6H_4OMe\text{-}p)(\mu\text{-}CF_3C_2CF_3)$, 110294-84-3; $(\eta\text{-}C_5H_5)_2Rh_2\{\mu\text{-}\eta^3\text{-}N(C_6H_4OMe\text{-}p)C(O)C(CF_3)C(CF_3)\}$, 110294-88-7; $(\eta\text{-}C_5H_5)_2Rh_2\{\mu\text{-}\eta^3\text{-}N(C_2H_5)C(O)C(CF_3)C(CF_3)\}$, 110294-89-8; $(\eta\text{-}C_5H_5)_2Rh_2\{\mu\text{-}\eta^3\text{-}N(C_6H_3Me_2\text{-}2,6)C(O)C(CF_3)C(CF_3)\}$, 110294-90-1; $(\eta\text{-}C_5H_5)_2Rh_2\{\mu\text{-}\eta\text{-}N(C_6H_4NO_2\text{-}p)C(O)C(CF_3)C(CF_3)\}$, 110294-91-2; $(\eta\text{-}C_5H_5)_2Rh_2(CO)(CNC_6H_4NO_2\text{-}p)(\mu\text{-}CF_3C_2CF_3)$, 110294-83-2; C_2H_5NCO, 624-79-3; $i\text{-}PrNCO$, 598-45-8; CyNCO, 931-53-3; $2,6\text{-}Me_2C_6H_4NCO$, 2769-71-3; MeNCO, 624-83-9; $t\text{-}BuNCO$, 1609-86-5; $(\eta\text{-}C_5H_5)_2Rh_2(CO)(CN\text{-}t\text{-}Bu)(\mu\text{-}CF_3C_2CF_3)$, 71853-17-3; $(\eta\text{-}C_5H_5)_2Rh_2(CO)(PPh_3)(\mu\text{-}CF_3C_2CF_3)$, 110351-10-5.

Supplementary Material Available: Tables of thermal parameters, ligand geometries, and equations for planes for $(\eta\text{-}C_5H_5)_2Rh_2(CO)(CNC_6H_3Me_2\text{-}2,6)(CF_3C_2CF_3)$ (4 pages); a listing of structure factor amplitudes (13 pages). Ordering information is given on any current masthead page.

Addition of Small Molecules to $(\eta\text{-}C_5H_5)_2Rh_2(CO)(CF_3C_2CF_3)$. 8.[1] Solution Behavior of the Isocyanide Complexes $(\eta\text{-}C_5H_5)_2Rh_2(CO)(CNR)(CF_3C_2CF_3)$ and Their Conversion to $(\eta\text{-}C_5H_5)_2Rh_2(CO)\{C(NR)C(CF_3)C(CF_3)\}$. Crystal and Molecular Structure of $(\eta\text{-}C_5H_5)_2Rh_2(CO)\{C(NEt)C(CF_3)C(CF_3)\}$

Ron S. Dickson,* Gary D. Fallon, Rhonda J. Nesbit, and Helen Pateras

Department of Chemistry, Monash University, Clayton, Victoria 3168, Australia

Received March 25, 1987

Coordinative addition of isocyanides CNR to $(\eta\text{-}C_5H_5)_2Rh_2(\mu\text{-}CO)(\mu\text{-}CF_3C_2CF_3)$ gives $(\eta\text{-}C_5H_5)_2Rh_2(CO)(CNR)(\mu\text{-}CF_3C_2CF_3)$ (1) which isomerizes in solution when R = Et, *i*-Pr, Cy, Ph, $p\text{-}MeOC_6H_4$, or $p\text{-}NO_2C_6H_4$ to **2**. Spectroscopic analysis establishes that **2** can be formulated as $(\eta\text{-}C_5H_5)_2Rh_2(CO)\{\mu\text{-}C(NR)C(CF_3)C(CF_3)\}$ and that it exists as a mixture of three interconverting isomers **2a**, **2b**, and **2c** in solution. The rate of interconversion between the various isomers has been investigated by variable-temperature NMR and varies according to R, being greatest for the aryl systems. The isomer distribution **2a**:**2b**:**2c** is both solvent- and temperature-dependent. The molecular structure of **2a**, R = Et, has been determined by X-ray crystallography. Crystal data: $C_{18}H_{15}F_6NORh_2$, M_r 581.2, monoclinic, $P2_1/n$, a = 14.636 (8) Å, b = 11.277 (6) Å, c = 11.774 (6) Å, β = 92.86 (9)°, Z = 4, final R = 0.056 for 2771 "observed" reflections. A bridging allylimine ligand and a terminal carbonyl are indicated for this isomer in the solid state. The reaction kinetics for the isomerization of **1** to **2** have been determined from NMR data. The rate of isomerization depends markedly on R and follows the sequence R = Cy ($t_{1/2}$ = 1740 min) < *i*-Pr < Ph < $p\text{-}MeOC_6H_4$ < $p\text{-}NO_2C_6H_4$ ($t_{1/2}$ = 1.4 min). The interconversion rates between isomers of **2** follow the same sequence.

Introduction

We have shown previously that the coordinative addition of ligands to $(\eta\text{-}C_5H_5)_2Rh_2(\mu\text{-}CO)(\mu\text{-}CF_3C_2CF_3)$ is frequently followed by facile intramolecular reactions between the added ligand and the coordinated hexafluorobutyne. The formation of bridging pentadienones,[2,3] bridging acrylamides,[4] and bridging allyl groups[5] when alkynes, isocyanates, and carbenes, respectively, are added provides examples of this type of behavior. As indicated in a previous paper,[1] the addition of isocyanides, CNR, to $(\eta\text{-}C_5H_5)_2Rh_2(\mu\text{-}CO)(\mu\text{-}CF_3C_2CF_3)$ results in the formation of $(\eta\text{-}C_5H_5)_2Rh_2(CO)(CNR)(\mu\text{-}CF_3C_2CF_3)$ which in many instances rapidly convert to isomeric species. In this paper, we unravel the nature of these isomeric species, and we describe the solution behavior of the systems.

Experimental Section

The general procedures and instrumentation used are described in the previous paper.[1] Literature procedures[6] were followed in preparing the following isocyanide ligands: PhNC, $p\text{-}MeOC_6H_4NC$, $p\text{-}NO_2C_6H_4NC$.

Formation of $(\eta\text{-}C_5H_5)_2Rh_2(CO)\{\mu\text{-}C(NR)C(CF_3)C(CF_3)\}$. The preparation of $(\eta\text{-}C_5H_5)_2Rh_2(CO)(CNR)(\mu\text{-}CF_3C_2CF_3)$ from $(\eta\text{-}C_5H_5)_2Rh_2(\mu\text{-}CO)(\mu\text{-}CF_3C_2CF_3)$ and CNR in dichloromethane at 20 °C has been described previously.[1] When left in solution (CH_2Cl_2, 20 °C), these complexes undergo structural rearrangements to give new species $(\eta\text{-}C_5H_5)_2Rh_2(CO)\{\mu\text{-}C(NR)C(CF_3)C(CF_3)\}$. The combined yield of $(\eta\text{-}C_5H_5)_2Rh_2(CO)(CNR)(\mu\text{-}CF_3C_2CF_3)$ and $(\eta\text{-}C_5H_5)_2Rh_2(CO)\{\mu\text{-}C(NR)C(CF_3)C(CF_3)\}$ is generally between 90 and 100%, and the proportion of the two isomers depends upon the age of the solution. The two complexes were separated by TLC (20 × 20 cm plates, 1:1 silica gel G–HF_{254} mixture as adsorbent, plates dried at room temperature only),

(1) Part 7: Bixler, J. W.; Bond, A. M.; Dickson, R. S.; Fallon, G. D.; Nesbit, R. J.; Pateras, H. *Organometallics*, preceding paper in this issue.
(2) Baimbridge, C. W.; Dickson, R. S.; Fallon, G. D.; Grayson, I.; Nesbit, R. J.; Weigold, J. *Aust. J. Chem.* **1986**, *39*, 1187.
(3) Dickson, R. S.; Fallon, G. D.; McLure, F. I.; Nesbit, R. J. *Organometallics* **1987**, *6*, 215.
(4) Dickson, R. S.; Nesbit, R. J.; Pateras, H.; Baimbridge, W.; Patrick, J. M.; White, A. H. *Organometallics* **1985**, *4*, 2128.
(5) Dickson, R. S.; Fallon, G. D.; Nesbit, R. J.; Pain, G. N. *Organometallics* **1985**, *4*, 355.
(6) Shingaki, T.; Takebayashi, M. *Bull. Chem. Soc. Jpn.* **1963**, *36*, 617.

0276-7333/87/2306-2517$01.50/0